Wolf-Rayet Stars
W.-R. Hamann, A. Sander, H. Todt, eds.
Potsdam: Univ.-Verlag, 2015
URL: http://nbn-resolving.de/urn:nbn:de:kobv:517-opus4-84268

High Resolution X-Ray Spectra of WR 6

D. Huenemoerder[1], K. Gayley[2], W.-R. Hamann[3], R. Ignace[4], J. Nichols[5], L. M. Oskinova[3], A. M. T. Pollock[6], N. Schulz[1]
[1]*MIT Kavli Institute*; [2]*Univ. Iowa*; [3]*Univ. Potsdam*; [4]*East Tennessee State Univ.*; [5]*Smithosonian Astrophysical Obs.*; [6]*ESA, & University of Sheffield*

As WR 6 is a putatively single WN4 star, and is relatively bright ($V = 6.9$), it is an ideal case for studying the wind mechanisms in these extremely luminous stars. To obtain higher resolution spectra at higher energy (above 1 keV) than previously obtained with the XMM/Newton RGS, we have observed WR 6 with the Chandra High Energy Transmission Grating Spectrometer for 450 ks. We have resolved emission lines of S, Si, Mg, Ne, and Fe, which all show a "fin"-shaped profile, characteristic of a self-absorbed uniformly expanding shell. Steep blue edges gives robust maximal expansion velocities of about 2000 km/s, somewhat larger than the 1700 km/s derived from UV lines. The He-like lines all indicate that X-ray emitting plasmas are far from the photosphere – even at the higher energies where opacity is lowest – as was also the case for the longer wavelength lines observed with XMM-Newton/RGS. Abundances determined from X-ray spectral modeling indicate enhancements consistent with nucleosynthesis. The star was also variable in X-rays and in simultaneous optical photometry obtained with *Chandra* aspect camera, but not coherently with the optically known period of 3.765 days.

1 Introduction

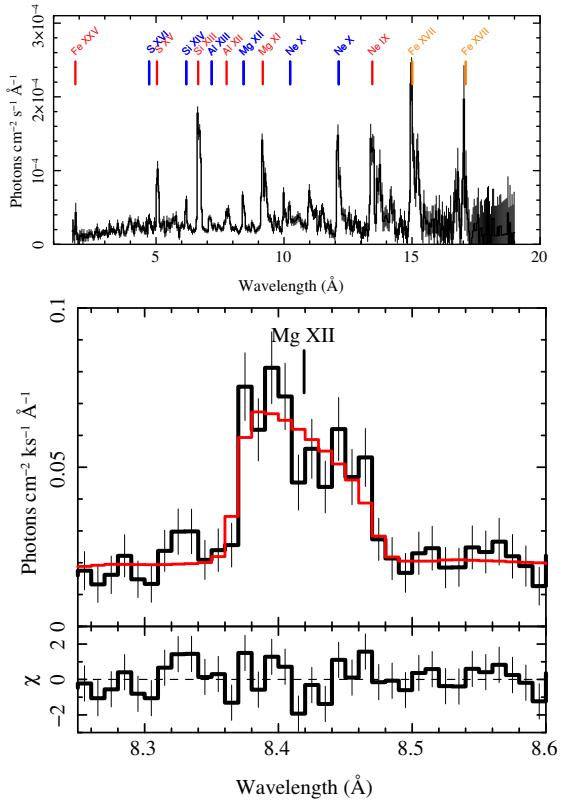

Fig. 1: The HETG spectrum (top) shows lines from H- (blue) and He-like (red) as well as Fe L-shell lines (orange). The lines have a "fin"-shaped profile (bottom) implying constant spherical expansion, as fit (red) to the Mg XII line (black), whose center is labeled. Residuals are shown in the lower sub-panel.

Wolf-Rayet stars are among the most massive and luminous of stars, whose rapid, dense winds and ultimate supernova detonations can contribute significantly to interstellar medium energetics, dynamics, and composition on large scales. Hence it is important to understand their winds and mass-loss rates. Such is usually done through optical and UV spectroscopy (Hamann et al. 2006; Hillier & Miller 1998). X-rays also tell an important story because supersonic winds can generate high temperature shocks. X-ray line strengths and profiles are key diagnostics of high energy processes occurring in the winds of WR-stars.

Hot star winds are thought to be the product of line-driven radiation pressure and dynamical instabilities which occur within the the acceleration zone which extends a few stellar radii above the photosphere (Lucy & White 1980; Krtička et al. 2009). This leads to broad lines (Ignace 2001; Owocki & Cohen 2001), and exposure to UV-intense radiation can destroy He-like forbidden lines, giving a valuable diagnostic on X-ray source location (Blumenthal et al. 1972; Waldron & Cassinelli 2001).

WR stars' massive winds are also thought to be line-driven and to have embedded shocks (Gayley & Owocki 1995). The high mass-loss rates, coupled with more compact distance scales and similar wind velocities as O-stars ($\sim 1000\,\mathrm{km\,s^{-1}}$), implies that WR stars have much denser winds than O stars, leading to higher optical depth, a feature we exploited in our analysis of X-ray profiles.

2 Characteristics of WR 6

WR 6 (EZ CMa), spectral type WN 4, is visually bright ($V = 6.9$; van der Hucht 2001), and has a distance of 1.8 kpc (Howarth & Schmutz 1995). There is no detectable trace of hydrogen in its atmo-

sphere and wind (Hamann & Koesterke 1998). WR 6 has a well established and consistent photometric period of 3.7650 d, though the modulation itself is highly variable in amplitude and phase (Georgiev et al. 1999; Robert et al. 1992; Lamontagne et al. 1986). Based on its radio and X-ray properties (Dougherty & Williams 2000; Oskinova 2005; Skinner et al. 2002), the star is considered to be single, and is not suspected of having a magnetically confined wind since it has no detected global magnetic field (de la Chevrotière et al. 2013). Other fundamental parameters of WR 6 can be found in Hamann et al. (2006).

3 Observations & Analysis

We observed WR 6 with the Chandra/HETG spectrometer (Canizares et al. 2005) in 2013 for a total of 440 ks (dataset identifiers 14533–5). The spectra cover the range from 1–30 Å with resolving powers ranging from 100 to 1000 (depending on wavelength and grating type). The data were reprocessed with standard CIAO programs (Fruscione et al. 2006, version 4.6) to apply the most recent calibrations (calibration database, version 4.5.9). Figure 1 (top panel) shows an overview of the flux spectrum.

The lines are fully resolved and appear non-Gaussian. For WR winds it is natural to expect line profiles that sample the asymptotic flow, because the winds are quite dense such that continuum optical depth unity in photoabsorption of X-ray emission is expected to be at relatively large radii. We have adopted the analytic line profile form valid in the limit of $\tau_c \gg 1$ from Ignace (2001): $f(w_z) = f_0 \left(\sqrt{1-w_z^2}\,/\arccos(-w_z)\right)^{1+q}$ where f_0 is a normalization constant and the dimensionless scaled velocity along the line-of-sight is $w_z = (c/v_\infty)(\lambda/\lambda_0 - 1)$ for a line having rest wavelength λ_0. We assumed that the emissivity per volume varies as density squared (i.e., collisional ionization equilibrium), but introduced an additional term in the form of r^{-q} ($q > -1$), which serves to modify the shape of the profile from a pure density squared case in order to represent a number of possible effects, such as a volume filling factor or an X-ray temperature distribution that depend on radius. Different q values are allowed for different lines. Figure 1 (bottom panel) shows a fit to Mg XII, a strong, relatively isolated line. All the lines share this shape, yielding a robust value for $v_\infty = 1950 \pm 20\,\mathrm{km\,s^{-1}}$. There is no trend with wavelength in contrast to that seen very strongly in thinner OB-star winds (e.g., ζ Oph Cassinelli et al. 2001). There is a hint of a trend for q with wavelength, largely driven by the RGS, but otherwise consistent with $q = -0.3 \pm 0.1$.

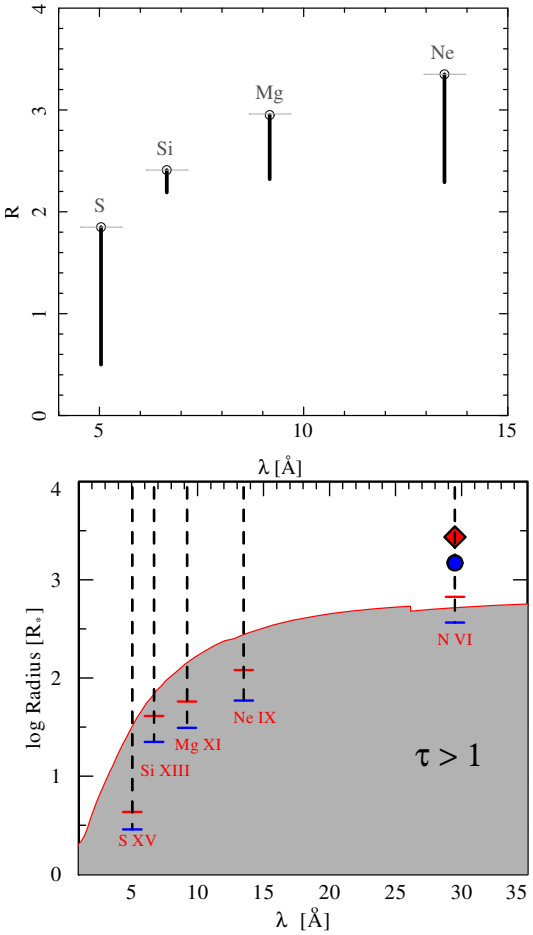

Fig. 2: The He-like $R = f/i$ ratios (top) are at their theoretically maximum values. Black bars show 90% confidence lower limits. Derived radii (bottom) for the lower limits under assumptions of localized (upper red bars) or distributed (lower blue bars) emission are all at large radii. The gray region shows where the continuum opacity exceeds 1. The N VI value is from XMM/Newton RGS, which also has fit results below the maximal R (diamond and circle).

The He-like line ratios are sensitive to UV photoexcitation and can be used to estimate the radii where X-rays are formed (Gabriel & Jordan 1969; Blumenthal et al. 1972; Waldron & Cassinelli 2007). Figure 2 shows our measurements of the R-ratio (forbidden to intercombination flux ratio, or f/i) for several ions (top panel). The best fit values are all at the un-photoexcited limit, indicating that X-rays are emitted far from the intense UV field. Using the 90% confidence limits in conjunction with a detailed model atmosphere for WR 6 of Hamann & Gräfener (2004) we determined the minimum radii of formation (Figure 2 lower panel). These are also generally at large radii, assuming either that the X-rays all form at one radius, or that they are distributed

above some onset radius.

While global modeling of the X-ray spectrum is difficult, due to the presence of both emission and absorption distributed in a likely clumpy wind, our provisional absorbed APEC model is useful in characterizing the X-ray spectrum. We added to the model of Oskinova et al. (2012) a higher temperature component apropos of the higher hard sensitivity of HETG. Comparing model and data revealed large residuals in *both* the Na X and Na XI regions which we could only reduce through a large enhancement ($\sim 7\times$) of the Na abundance. Figure 3 shows this spectral region and our fit. We could not explain the residuals by Fe blends, nor weak lines found in other spectra but not in the atomic database. We conclude that Na is indeed enhanced, and we suggest that this is a result of the Ne-Na nuclear cycle (Cavanna et al. 2014) and is diagnostic of the evolved state of WR 6.

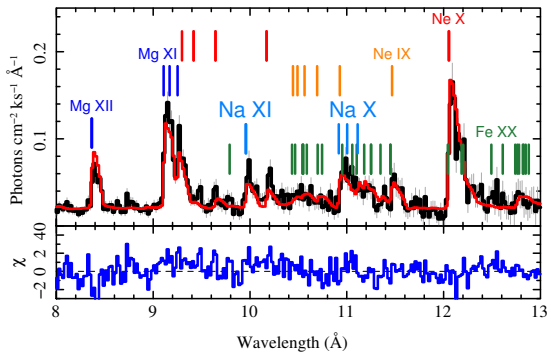

Fig. 3: To fit the HETG spectrum in the 10Å region, we required an enhanced Na abundance by about a factor of 7. We show the observed spectrum (black) and a 4-temperature APEC model (red), and residuals (blue). Some line positions are marked at the blue edge of the profile, and have vertical offsets and color-coding by element and ion (or in the case of Fe, several ions from XVII – XXIV are included).

4 Conclusions

The line profiles are consistent with production of X-rays in an optically thick photoabsorbing wind from a region of constant spherical expansion, far outside the acceleration zone where embedded wind shocks are thought to effectively generate X-rays in OB-stars. In WR 6, we cannot observe this zone.

The He-like line ratios are consistent with the line profile modeling assumptions and localize the emergent emission throughout radii larger than 10–300 R_*.

Presence of enhanced Na lines is indicative of nucleosynthesis. X-ray spectra such as this may be a good way to probe evolutionary states through relative abundances of Ne, Na, Al, and Mg.

Acknowledgements: This work was supported by NASA through the Smithsonian Astrophysical Observatory under contract NAS8-03060 via Chandra Awards GO3-14003A and GO5-16009A to MIT (DPH), GO3-14003D to ETSU (RI), GO3-14003B to SAO (JN), and GO3-13003C to UI (KGG). LO thanks the DLR grant 50 OR 1302.

References

Blumenthal, G. R., Drake, G. W. F., & Tucker, W. H. 1972, ApJ, 172, 205
Canizares, C. R., Davis, J. E., Dewey, D., et al. 2005, PASP, 117, 1144
Cassinelli, J. P., Miller, N. A., Waldron, W. L., MacFarlane, J. J., & Cohen, D. H. 2001, ApJ, 554, L55
Cavanna, F., Depalo, R., Menzel, M.-L., et al. 2014, European Physical Journal A, 50, 179
de la Chevrotière, A., St-Louis, N., Moffat, A. F. J., & the MiMeS Collaboration. 2013, ApJ, 764, 171
Dougherty, S. M. & Williams, P. M. 2000, MNRAS, 319, 1005
Fruscione, A., McDowell, J. C., Allen, G. E., et al. 2006, in Presented at the Society of Photo-Optical Instrumentation Engineers (SPIE) Conference, Vol. 6270, SPIE Conference Series
Gabriel, A. H. & Jordan, C. 1969, MNRAS, 145, 241
Gayley, K. G. & Owocki, S. P. 1995, ApJ, 446, 801
Georgiev, L. N., Koenigsberger, G., Ivanov, M. M., St.-Louis, N., & Cardona, O. 1999, A&A, 347, 583
Hamann, W.-R. & Gräfener, G. 2004, A&A, 427, 697
Hamann, W.-R., Gräfener, G., & Liermann, A. 2006, A&A, 457, 1015
Hamann, W.-R. & Koesterke, L. 1998, A&A, 333, 251
Hillier, D. J. & Miller, D. L. 1998, ApJ, 496, 407
Howarth, I. D. & Schmutz, W. 1995, A&A, 294, 529
Ignace, R. 2001, ApJ, 549, L119
Krtička, J., Feldmeier, A., Oskinova, L. M., Kubát, J., & Hamann, W.-R. 2009, A&A, 508, 841
Lamontagne, R., Moffat, A. F. J., & Lamarre, A. 1986, AJ, 91, 925
Lucy, L. B. & White, R. L. 1980, ApJ, 241, 300
Oskinova, L. M. 2005, MNRAS, 361, 679
Oskinova, L. M., Gayley, K. G., Hamann, W.-R., et al. 2012, ApJ, 747, L25
Owocki, S. P. & Cohen, D. H. 2001, ApJ, 559, 1108
Robert, C., Moffat, A. F. J., Drissen, L., et al. 1992, ApJ, 397, 277
Skinner, S. L., Zhekov, S. A., Güdel, M., & Schmutz, W. 2002, ApJ, 579, 764
van der Hucht, K. A. 2001, New A Rev., 45, 135
Waldron, W. L. & Cassinelli, J. P. 2001, ApJ, 548, L45
Waldron, W. L. & Cassinelli, J. P. 2007, ApJ, 668, 456

D. John Hillier: Calculations by Prantzos et al (Prantzos, N., Doom, C., de Loore, C., & Arnould, M. 1986, ApJ, 304, 695) show that in LBVs and WN stars sodium can be enhanced by a factor of 2 to 4. This can probably explain the enhanced sodium derived from the X-ray spectrum of HD 50896 (WR6).

Michael Corcoran: The X-ray data show that the X-ray emission in WR 6 is far from the star, yet it's variable which suggests that it arises from a relatively small region far from the star. Any comments?

David Huenemoerder: The X-ray modulation is small (about 15%), and has similar amplitude in both the Chandra and XMM (Oskinova et al. 2012). data. The variability is not coherent in phase. We don't know what causes the variability, and are looking for time-resolved spectral changes in the high-resolution spectrum. There is an heuristic model invoking co-rotating interaction region (CIR) propagating spiral structures which can qualitatively describe this type of X-ray variability (Ignace et al. 2013).

Anthony (Tony) Moffat: According to the CIR models of Cranmer & Owocki (1996) the maximum shock velocities reach 500 km/s, so moderately hard X-rays only.

David Huenemoerder: Such a shock velocity would only be sufficient to produce soft X-rays ($\sim$ 2 MK). There is plasma at this temperature in EZ CMa, but there is also significantly hotter plasma, reaching about 40 MK.

Götz Gräfener: WR 6 shows line-depolarization which may indicate a wind anisotropy or DACs (Discrete Absorption Components). Do you think that the latter could explain the X-ray variability?

David Huenemoerder: Yes, possibly. But if related to DACs, coherent structures would need to exist far out in the X-ray emitting wind.

(Ignace et al. 2013 presented a phenomenological model using co-rotating interaction regions to qualitatively explain X-ray variability seen in the XMM observations of WR 6.)